MATERIALS SCIENCE / МАТЕРИАЛОВЕДЕНИЕ

UDC 669.539.382:669.17:6251
DOI 10.17073/0368-0797-2024-4-424-432

Original article
Оригинальная статья

PHYSICS OF HARDENING OF THE ROLLING SURFACE OF RAIL HEAD FROM HYPEREUTECTOID STEEL AFTER OPERATION

N. A. Popova[1], V. E. Gromov[2] ✉, A. B. Yur'ev[2], E. A. Martusevich[2], M. A. Porfir'ev[2]

[1] **Tomsk State University of Architecture and Building** (2 Solyanaya Sqr., Tomsk 634003, Russian Federation)
[2] **Siberian State Industrial University** (42 Kirova Str., Novokuznetsk, Kemerovo Region – Kuzbass 654007, Russian Federation)

✉ gromov@physics.sibsiu.ru

Abstract. In Russia, with its extensive railway system, for more than 5 years, special-purpose rails of increased wear resistance and contact endurance of the DH400RK category were produced from steel with a carbon content >0.8 %. On the head rolling surface of differentially hardened long rails made of hypereutectoid steel after long-term operation, transmission electron microscopy methods revealed the morphological components of the structure: lamellar pearlite, fragmented pearlite, destroyed lamellar pearlite, globular pearlite, completely destroyed pearlite, subgrain structure. The contribution of hardening due to: lattice friction, solid solution hardening, pearlite hardening, incoherent cementite particles, grain boundaries and subboundaries, dislocation substructure and internal stress fields were quantified. A hierarchy of these mechanisms was made and it was noted that for the fillet surface of the rail head, the main hardening mechanism is hardening by incoherent particles, as well as mechanisms caused by internal long-range (local) stresses, internal shear stresses ("forests" of dislocations) and substructural hardening. For the rolling surface along the central axis of the rail head, the main role in hardening belongs to long-range stress fields (especially its elastic component), hardening by incoherent particles and substructural hardening. Taking into account the volume fractions of the morphological components and their yield strength, the additive yield strength on the head rolling surface in the center and on the fillet was determined: 7950 and 2218 MPa, respectively. The paper presents a physical interpretation of the difference in values of the additive yield strength on the rolling surface of the rail head in the center and on the fillet.

Keywords: rolling surface, rails, fillet, hardening mechanisms, additive yield strength, hypereutectoid steel

Acknowledgements: The work was performed within the framework of the state task of the Ministry of Science and Higher Education of the Russian Federation (subject No. FEMN-2023-0003). The authors express their gratitude to E.V. Polevoi for the samples provided and to I.Y. Litovchenko for assistance in conducting TEM studies.

For citation: Popova N.A., Gromov V.E., Yur'ev A.B., Martusevich E.A., Porfir'ev M.A. Physics of hardening of the rolling surface of rail head from hypereutectoid steel after operation. *Izvestiya. Ferrous Metallurgy*. 2024;67(4):424–432. https://doi.org/10.17073/0368-0797-2024-4-424-432

ФИЗИКА УПРОЧНЕНИЯ ПОВЕРХНОСТИ КАТАНИЯ ГОЛОВКИ РЕЛЬСОВ ИЗ ЗАЭВТЕКТОИДНОЙ СТАЛИ ПОСЛЕ ЭКСПЛУАТАЦИИ

Н. А. Попова[1], В. Е. Громов[2] ✉, А. Б. Юрьев[2], Е. А. Мартусевич[2], М. А. Порфирьев[2]

[1] **Томский государственный архитектурно-строительный университет** (Россия, 634003, Томск, пл. Соляная, 2)
[2] **Сибирский государственный индустриальный университет** (Россия, 654007, Кемеровская обл. – Кузбасс, Новокузнецк, ул. Кирова, 42)

✉ gromov@physics.sibsiu.ru

Аннотация. В России с ее протяженной сетью железных дорог более пяти лет производятся рельсы специального назначения повышенной износостойкости и контактной выносливости категории ДТ400ИК из стали с содержанием углерода более 0,8 %. На поверхности катания головки дифференцированно закаленных длинномерных рельсов из заэвтектоидной стали после длительной эксплуатации (пропущенный тоннаж 187 млн т брутто на экспериментальном кольце) методами просвечивающей электронной микроскопии выявлены морфологические составляющие структуры: пластинчатый перлит, фрагментированный перлит, разрушенный пластинчатый перлит, глобулярный перлит, полностью разрушенный перлит, субзеренная структура. Проведена количественная оценка вкладов упрочнения, обусловленных трением кристаллической решетки, твердорастворным упрочнением, упрочнением за счет перлита, упрочнением некогерентными частицами цементита, границами зерен и субграницами, дислокационной субструктурой и внутренними полями напряжений. Установлена

иерархия этих механизмов и отмечено, что для поверхности скругления (выкружки) головки рельсов основным механизмом упрочнения является упрочнение некогерентными частицами, а также механизмы, обусловленные внутренними дальнодействующими (локальными) напряжениями, внутренними напряжениями сдвига («леса» дислокаций) и субструктурным упрочнением. Для поверхности катания по центральной оси головки рельсов основная роль в упрочнении принадлежит упрочнению дальнодействующими полями напряжений (особенно ее упругой компонентой), упрочнению некогерентными частицами и субструктурному упрочнению. С учетом объемных долей морфологических составляющих и их предела текучести определен аддитивный предел текучести на поверхности катания по центру головки и выкружке. Он составил 7950 и 2218 МПа для центра головки и выкружки. Представлена физическая интерпретация различия значений аддитивного предела текучести на поверхности катания головки рельсов в центре и на выкружке.

Ключевые слова: поверхность катания, рельсы, выкружка, механизмы упрочнения, аддитивный предел текучести, заэвтектоидная сталь

Благодарности: Работа выполнена в рамках государственного задания Министерства науки и высшего образования Российской Федерации (тема № FEMN-2023-0003). Авторы выражают благодарность Е.В. Полевому за предоставленные образцы, И.Ю. Литовченко за помощь в проведении ПЭМ-исследований.

Для цитирования: Попова Н.А., Громов В.Е., Юрьев А.Б., Мартусевич Е.А., Порфирьев М.А. Физика упрочнения поверхности катания головки рельсов из заэвтектоидной стали после эксплуатации. *Известия вузов. Черная металлургия*. 2024;67(4):424–432. https://doi.org/10.17073/0368-0797-2024-4-424-432

Introduction

Rails are predominantly removed from service due to contact fatigue damage and surface wear [1; 2]. In recent years, with increasing railway traffic speeds and axle loads, the operational durability requirements for rails have become more demanding [3 – 5]. From both practical and fundamental perspectives, the development of special-purpose rails with enhanced performance characteristics is of significant importance [6 – 8]. In Russia, home to one of the world's longest railway networks, this challenge has been addressed since 2018 through the production of long, differentially hardened rails with improved wear resistance and contact fatigue strength, classified as DT400IK [9]. These rails are manufactured from steel containing more than 0.8 wt. % carbon, which ensures the formation of a subgrain structure with a high density of low-angle boundaries in the surface layer. Modern physical materials science techniques, particularly transmission electron microscopy [10 – 12], are employed to monitor changes in structure, phase composition, and defect substructure that lead to the degradation of mechanical properties [13 – 15]. Improving the technology for special-purpose rail production and ensuring high-performance properties requires a deep understanding of the physical nature and evolution trends of the structural-phase states and fine substructure in the surface layers of rails [16 – 18]. Such data are crucial for reliably achieving the target of transporting up to 2 billion tons [19 – 21]. Analysis conducted on rails made of hypoeutectoid steel with carbon content below 0.8 wt. % – as presented in [22 – 25] – has enabled the quantification of physical hardening mechanisms, the establishment of their hierarchy, and the determination of overall yield strength. However, there is a notable lack of studies focused on rails made of hypereutectoid steel.

The objective of this study is to compare the deformation hardening mechanisms of the rolling surface and fillet of special-purpose DH400RK rails after they have been in operation on the Russian Railways (RZD) test circuit at Scherbinka, following a tonnage of 187 million tons (gross).

Materials and methods

The internal structure and phase composition were studied on samples of differentially hardened DH400RK category rails, made from E0.9C–Cr–N–V–Fe grade steel produced by EVRAZ ZSMK, after they had undergone a tonnage of 187 million tons (gross) at the Russian Railways (RZD) test circuit. The chemical composition of E90HAF rail steel, according to GOST 5185 – 2013 and TS 24.10.75111-298-057576.2017, included the following main elements, wt. %: 0.92 C, 0.4 Si, 1.0 Mn, 0.3 Cr, 0.14 V, with iron as the base. The mechanical properties are as follows: yield strength – over 900 MPa, tensile strength – 1350 MPa. relative elongation – 9.0 %, relative reduction – 18 %, impact toughness – 15 J/cm^2, and hardness on the rolling surface of the rail head – 400 – 450 HB.

The rolling surface and fillet of the rail head were investigated (Fig. 1) using transmission electron microscopy (TEM) on thin foils with a JEM-2100 electron microscope (Jeol, Japan) [26 – 28].

To evaluate the hardening mechanisms that contribute to the yield strength in the studied steel, each sample was analyzed for structural morphological features, phase composition, and fine structure parameters, including the volume fractions of morphological constituents P_v. The localization of the carbide phase (cementite) was identified, and for each specific location, the shape, size (d), particle spacing (r), and volume fraction (δ) of the particles were determined. In each morphological component, as well as in the material as a whole, the scalar ρ and excessive $\rho_{\pm}$ dislocation densities were calculated, along with the amplitudes of internal stresses generated by them – namely, shear stresses (σ_f, or "forests"

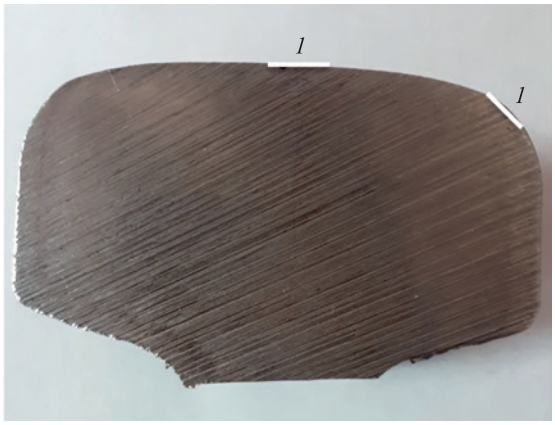

Fig. 1. Schematic representation of a rail sample after passing a tonnage of 187 million tons, indicating the places used to study the structure:
1 – rolling surfaces and rounding of the rail head (fillet)

Рис. 1. Схематическое изображение образца рельса после пропущенного тоннажа 187 млн т с указанием мест, использованных для исследования структуры:
1 – поверхности катания и скругления головки рельса (выкружки)

of dislocations) and long-range stresses (σ_l), which arise in regions with an excess dislocation density. All quantitative parameters of the fine structure were measured within each morphological component and statistically processed, with the mean values presented in Table 1 (where D_l represents the fragment or subgrain size; χ, χ_{pl} and χ_{el} represent the curvature-torsion amplitude of the crystal lattice and its plastic and elastic components, respectively; σ_l^{pl} and σ_l^{el} are the amplitudes of internal long-range stresses and their plastic and elastic components.

The technique for determining these quantitative parameters is detailed in [9; 29].

Results and discussion

The studies have shown that regardless of the location on the rail head surface (Fig. 1) the following morphological components are observed in the structure: lamellar (ideal) pearlite with parallel alternating lamellae of ferrite and cementite; fragmented lamellar pearlite, in which dislocation walls across the di-rection of α-phase plates are formed; destroyed lamellar perlite with bent, cut and crushed Fe_3C lamellae; globular pearlite in the form of grains with globular Fe_3C particles, subgrain structure – small equiaxed fragments with cementite particles along the boundaries and in the junctions. The images of these morphological components are consistent with those observed for rails made of hypoeutectoid steel, as shown in [1].

A different type of structure was identified on the fillet surface – a completely destroyed structure. This structure, characterized by completely destroyed pearlite colonies,

Table 1. **Quantitative parameters of the structure of hypereutectoid rail steel on the rounding surface of the rail head (fillet)**

Таблица 1. **Количественные параметры структуры заэвтектоидной рельсовой стали на поверхности скругления головки рельса (выкружки)**

Parameters		Perlite				Destroyed structure	Subgrain structure
		ideal	fragmented	destroyed	globular		
P_v, %		5	20	10	3	60	2
D_l, nm		–	80×125	–	–	–	90
$\rho \cdot 10^{-10}$, cm^{-2}		6.5	4.3	4.5	3.0	6.6	1.4
σ_f, MPa		510	415	425	345	515	235
$\chi = \chi_{pl} + \chi_{el}$, cm^{-1}		765 + 0	1075 + 75	805 + 0	740 + 0	1650 + 95	350 + 390
$\rho_{\pm} \cdot 10^{-10}$, cm^{-2}		3.1	4.3	3.2	3.0	6.6	1.4
$\sigma_l = \sigma_l^{pl} + \sigma_l^{el}$, MPa		350 + 0	415 + 120	355 + 0	345 + 0	515 + 150	235 + 625
Fe_3C (at the boundaries)	*d*, nm	–	15×95	–	–	–	5×35
	r, nm	–	105	–	–	–	85
	δ, %	–	0.7	–	–	–	0.05
Fe_3C (inside)	*d*, nm	15	5×15	20×110	45	8×30	–
	r, nm	80	40	120	100	40	–
	δ, %	12.0	0.1	1.2	2.3	0.4	0
Fe_3C (at subgrain junctions)	*d*, nm	–	–	–	–	–	20
	r, nm	–	–	–	–	–	115
	δ, %	–	–	–	–	–	0.15

contains small, chaotically arranged carbide particles (Fe_3C) with an acicular shape and a high scalar dislocation density (Fig. 2, *a*).

The material on the rolling surface in the head center predominantly consists of a subgrain structure (90 %) (Fig. 2, *b*), while this structure accounts for only 2 % of the fillet surface. The research demonstrated that, in all morphological components, the dislocation structure type remains consistent: the dislocation substructure is represented by dense dislocation arrays. In all morphological components, there are bend extinction contours, originating from interfaces of pearlite grains and colonies, cementite plates in pearlite grains, fragment and subgrain boundaries, carbide particles (cementite) of lamellar and rounded shapes located on the boundaries and within the dislocation fragments and subgrains, junctions of subgrains, and the dislocation substructure.

Calculations presented in [9] indicate that, in the fillet surface layer, within the ideal, destroyed, and globular pearlite, the scalar density of dislocations ρ is higher than the excess density of dislocations $\rho_{\pm}$, as determined from the width of the bend extinction contours (Table 1), meaning that $\rho > \rho_{\pm}$ and, accordingly, $\sigma_l < \sigma_f$. This indicates that the curvature-twist of the crystal lattice in these morphological components is purely plastic in nature. In fragmented pearlite, as well as in completely destroyed and subgrain structures, the value ρ is smaller than the calculated value of $\rho_{\pm}$, meaning $\rho < \rho_{\pm}$ and, $\sigma_f < \sigma_l$, which implies that the curvature-twist of the crystal lattice in these components is elastic-plastic in nature. However, in fragmented pearlite and completely destroyed structures $\chi_{pl} \gg \chi_{el}$, whereas in the subgrain structure $\chi_{pl} \approx \chi_{el}$ (Table 1).

In the surface layer of the rail head center, the value ρ in all morphological components was found to be smaller than the value of $\rho_{\pm}$ calculated based on the width of extinction contours [9] (Table 2). This indicates that the curvature-twist of the crystal lattice in all morphological components is elastic-plastic, with $\chi = \chi_{pl} + \chi_{el}$. In the subgrain structure, which occupies the majority of the material, χ_{el} is nearly three times greater than χ_{pl}.

In the surface layer of the rail head, elastic-plastic curvature-twist of the crystal lattice is observed across all morphological components. Notably, in the subgrain structure, which makes up 90 % of the material, the values of χ and σ_l are the highest, while the value of σ_{pl} is more than an order of magnitude smaller than that of σ_{el} (Table 2). This explains the presence of microcracks in these areas.

The quantitative results presented in Tables 1 and 2 served as the basis for calculating the additive (total) yield strength in each morphological component and for the material as a whole. It is important to note that individual mechanisms contribute differently to overall strengthening, as these are influenced by various factors in each case [30 – 32]. Therefore, when estimating the additive yield strength σ_{ad}, it is crucial to consider the volume fractions P_v of each morphological component σ_i

$$\sigma = \sum P_i \sigma_i,$$

where P_i and σ_i are volume fractions and yield strength of each morphological component of the structure.

Previously, it was assumed that the additive yield strength could be determined by simply summing the contributions of individual hardening mechanisms [30]. However, it has now been demonstrated that, in some cases, these values should be summed using a quadratic approximation [31; 32]. This approach is particularly relevant for the mechanisms $\Delta\sigma_f$ and $\Delta\sigma_g$, which act locally and inhomogeneously within the grains. Thus,

$$\sigma_{ad} = \Delta\sigma_p + \Delta\sigma_s + \Delta\sigma_g + \Delta\sigma_{or} + \Delta\sigma_{perl} + \\ + \Delta\sigma_{ss} + \sqrt{\Delta\sigma_f^2 + \Delta\sigma_l^2},$$

where $\Delta\sigma_n = 35$ MPa [9] represents the friction stress of dislocations in the crystal lattice of α-iron; $\Delta\sigma_s$ refers

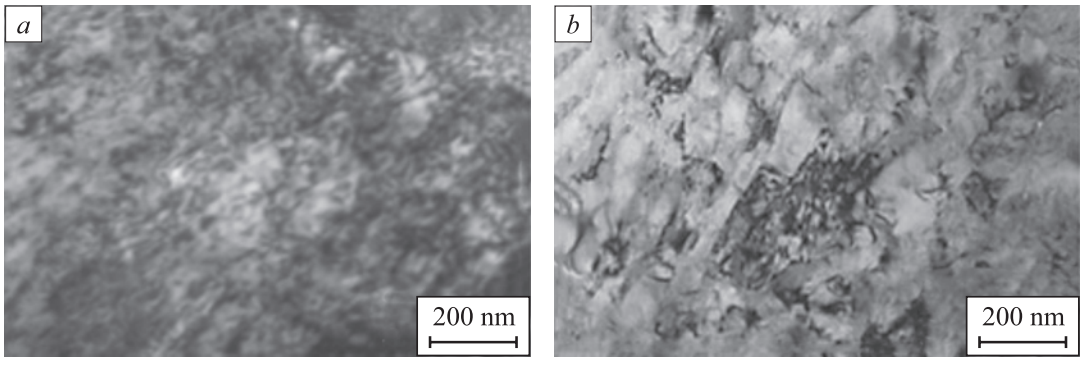

Fig. 2. TEM images of a completely destroyed (*a*) and subgrain structure (*b*)

Рис. 2. ПЭМ-изображения полностью разрушенной (*a*) и субзеренной структуры (*b*)

Table 2. **Parameters of the fine structure of pearlite in the rolling surface center**

Таблица 2. **Параметры тонкой структуры перлита в центре поверхности катания**

Parameters		Perlite				Subgrain structure
		ideal	fragmented	destroyed	globular	
P_v, %		~1	10	0	0	90
D_1, nm		–	50×160	–	–	80
$\rho \cdot 10^{-10}$, cm^{-2}		8.3	5.0	–	–	3.6
σ_f, MPa		575	445	–	–	380
$\chi = \chi_{pl} + \chi_{el}$, cm^{-1}		2075 + 25	1250 + 1430	–	–	900 + 2660
$\rho_{\pm} \cdot 10^{-10}$, cm^{-2}		8.3	5.0	–	–	3.6
$\sigma_l = \sigma_l^{pl} + \sigma_l^{el}$, MPa		575 + 40	445 + 2280	–	–	380 + 4255
Fe_3C (at the boundaries)	*d*, nm	–	15	–	–	15
	r, nm	–	40	–	–	30
	δ, %	–	0.6	–	–	1.0
Fe_3C (inside)	*d*, nm	15×20	15	–	–	10
	r, nm	40	35	–	–	35
	δ, %	1.1	0.7	–	–	0.2
Fe_3C (at subgrain junctions)	*d*, nm	–	–	–	–	20
	r, nm	–	–	–	–	100
	δ, %	–	–	–	–	0.01

to solid solution hardening (the hardening of ferrite solid solution by dissolved alloying elements); $\Delta\sigma_g$ denotes grain boundary hardening (due to grain boundaries); $\Delta\sigma_{or}$ is the hardening of material by incoherent particles as dislocations bypass them via the Orowan mechanism; $\Delta\sigma_{perl}$ represents hardening due to pearlitic component (barrier inhibition within pearlitic colonies); $\Delta\sigma_{ss}$ refers to substructural hardening (due to intraphase boundaries) the formula contains no such values); $\Delta\sigma_f$ is the hardening by the "forest" of dislocations that cut glide dislocations (internal shear stress); and $\Delta\sigma_l$ represents hardening by long-range stress fields (internal moment or local stresses), with $\Delta\sigma_l = \Delta\sigma_{el} + \Delta\sigma_{pl}$, where $\Delta\sigma_{el}$ is the elastic component and $\Delta\sigma_{pl}$ is the plastic component of long-range stresses.

The contributions of these hardening mechanisms were qualitatively assessed using the formulas given in [29; 31; 32], and the results are presented in Tables 3 and 4.

The analysis of data from Tables 3 and 4 shows that the strength of the steel is multifactorial, with physical mechanisms that are cumulative in nature. For the fillet surface, the primary hardening mechanism is Orowan strengthening ($\Delta\sigma_{or}$). This is primarily because the completely destroyed structure occupies the majority (60 %) of the fillet surface. The contributions from long-range stress fields ($\Delta\sigma_g$) and the stresses from the "forest" of dislocations ($\Delta\sigma_f$) are also significant. The emerging subgrain structure forms numerous grain junctions, leading to an increase in the sources of extinction contours and, consequently, a growth in $\Delta\sigma_g$. However, since the volume fraction of the subgrain structure (P_v) is low (2 %), its contribution to the strengthening of the fillet surface is minimal. The strengthening is primarily due to the fragmented substructure and the completely destroyed structure. The additive yield strength at the fillet surface is 2218 MPa.

For the central part of the rolling surface of the rail head, the additive yield strength is much higher, reaching 7950 MPa. The main hardening mechanisms (Table 4) include strengthening by internal elastic local stresses, substructural strengthening, and strengthening by incoherent particles.

The significant difference in the values of additive yield strength ($\sigma_{ad}^{fillet} < \sigma_{ad}^{centr}$) can be explained by the fact that, in the head center's rolling surface, the volume fraction of the subgrain structure is 45 times higher than that in the fillet. The subgrains form in the nanometer size range, leading to a high density of sub-boundaries and junctions (primarily triple junctions) of subgrains, which are the sources of extinction contours (mainly elastic). These contours result in high values of internal long-range stresses, with the elastic component being more than an order of magnitude higher than the plastic one. This combination determines the final effect. On the fillet surface, the main morphological components are destroyed pearlite and a completely destroyed structure with low-density boundaries.

Table 3. **Contribution of various mechanisms to hardening of hypereutectoid rail steel in various morphological components and in general according to the material of the rounding surface of the rail head (fillet)**

Таблица 3. **Величины вкладов различных механизмов в упрочнение заэвтектоидной рельсовой стали в различных морфологических составляющих и в целом по материалу поверхности скругления головки рельса (выкружки)**

Contributions	Perlite				Destroyed structure	Subgrain structure	In the material
	ideal	fragmented	destroyed	globular			
P_v, %	5	20	10	3	60	2	100
$\Delta\sigma_p$, MPa	35	35	35	35	35	35	35
$\Delta\sigma_s$, MPa	80	180	80	80	150	90	142
$\Delta\sigma_g$, MPa	–	–	205	360	195	–	148
$\Delta\sigma_{perl}$, MPa	965	–	–	–	–	–	48
$\Delta\sigma_{ss}$, MPa	–	1465	–	–	–	1665	326
$\Delta\sigma_{or}$, MPa	–	1125	340	200	805	580	760
$\Delta\sigma_f$, MPa	510	415	425	345	515	235	475
$\Delta\sigma_{pl}$, MPa	350	415	355	345	515	235	467
$\Delta\sigma_{el}$, MPa	0	120	0	0	150	625	127
$\Delta\sigma_l$, MPa	350	535	355	345	665	860	587
$\sum\Delta\sigma_i$, MPa	1699	3482	1214	1163	2026	3261	2218
$\sum\Delta\sigma_i P_i$, MPa	85	696	121	35	1216	65	2218

Table 4. **Contribution of various mechanisms to hardening of rail steel in various morphological components and in general for the material in the rail head center**

Таблица 4. **Величины вкладов различных механизмов в упрочнение рельсовой стали в различных морфологических составляющих и в целом по материалу в центре головки рельса**

Contributions	Perlite				Subgrain structure	In the material
	ideal	fragmented	destroyed	globular		
P_v, %	~1	10	0	0	90	100
$\Delta\sigma_p$, MPa	35	35	–	–	35	35
$\Delta\sigma_s$, MPa	80	210	–	–	210	210
$\Delta\sigma_g$, MPa	–	–	–	–	–	0
$\Delta\sigma_{perl}$, MPa	1120	–	–	–	–	10
$\Delta\sigma_{ss}$, MPa	–	1430	–	–	1875	1830
$\Delta\sigma_{or}$, MPa	–	1070	–	–	1435	1400
$\Delta\sigma_f$, MPa	575	445	–	–	380	390
$\Delta\sigma_{pl}$, MPa	575	445	–	–	380	390
$\Delta\sigma_{el}$, MPa	40	2280	–	–	4255	4060
$\Delta\sigma_l$, MPa	615	2725	–	–	4635	4450
$\sum\Delta\sigma_i$, MPa	2077	5506	–	–	8206	7957
$\sum\Delta\sigma_i P_i$, MPa	21	551			7385	7957

Conclusions

Transmission electron microscopy was used to reveal the morphological components of the rolling surface of the rail head made of hypereutectoid steel, both at the center and in the fillet. The identified components include lamellar pearlite, fragmented pearlite, destroyed lamellar pearlite, globular pearlite, completely destroyed pearlite, and subgrain structure. We conducted a quantitative analysis of hardening mechanisms and assessed

the contributions from lattice friction, solid solution hardening, pearlite hardening, incoherent cementite particles, grain boundaries and sub-boundaries, dislocation substructure, and internal stress fields. For the fillet surface, we established that the main hardening mechanism is due to incoherent particles, along with mechanisms based on internal long-range (local) stresses, internal shear stresses ("forests" of dislocations), and substructural hardening.

For the central part of the rolling surface, the primary hardening mechanisms are long-range stress fields, incoherent particles, and substructural hardening. We determined the additive yield strength at the rolling surface and explained the difference in its values between the head center and the fillet.

References / Список литературы

1. Yur'ev A.A., Kuznetsov R.V., Gromov V.E., Ivanov Yu.F., Shlyarova Yu.A. Long Rails: Structure and Properties after Long-Term Operation. Novokuznetsk: Poligrafist; 2022:311. (In Russ.).

   Юрьев А.А., Кузнецов Р.В., Громов В.Е., Иванов Ю.Ф., Шлярова Ю.А. Длинномерные рельсы: структура и свойства после сверхдлительной эксплуатации. Новокузнецк: «Полиграфист»; 2022:311.
2. Shur E.A. Rails Damage. Moscow: Intekst; 2012:153. (In Russ.).

   Шур Е.А. Повреждения рельсов. Москва: Интекст; 2012:153.
3. Steenbergen M. Rolling contact fatigue: Spalling versus transverse fracture of rails. *Wear*. 2017;380-381:96–105. http://doi.org/10.1016/j.wear.2017.03.003
4. Skrypnyk R., Ekh M., Nielsen J.C.O., Palsson B.A. Prediction of plastic deformation and wear in railway crossings – Comparing the performance of two rail steel grades. *Wear*. 2019;428-429:302–314. http://doi.org/10.1016/j.wear.2019.03.019
5. Miranda R.S., Rezende A.B., Fonseca S.T., Fernandes F.M., Sinatora A., Mei P.R. Fatigue and wear behavior of pearlitic and bainitic microstructures with the same chemical composition and hardness using twin-disc tests. *Wear*. 2022; 494-495:204253. http://doi.org/10.1016/j.wear.2022.204253
6. Pereira H.B., Alves L.H.D., Rezende A.B., Mei P.R., Goldenstein H. Influence of the microstructure on the rolling contact fatigue of rail steel: Spheroidized pearlite and fully pearlitic microstructure analysis. *Wear*. 2022;498-499:204299. http://doi.org/10.1016/j.wear.2022.204299
7. Ivanov Yu.F., Porfir'ev M.A., Gromov V.E., Kryukov R.E., Shlyarova Yu.A. Structural and phase states in the head of special-purpose rails after prolonged operation. *Metally*. 2023;(6):53–58. (In Russ.). https://doi.org/10.31857/S086957332306006X

   Иванов Ю.Ф., Порфирьев М.А., Громов В.Е., Крюков Р.Е., Шлярова Ю.А. Структурно-фазовые состояния в головке рельсов специального назначения после длительной эксплуатации. *Металлы*. 2023;(6):53–58. https://doi.org/10.31857/S086957332306006X
8. Ivanisenko Yu., Fecht H.J. Microstructure modification in the surface layers of railway rails and wheels: Effect of high strain rate deformation. *Steel Tech*. 2008;3(1):19–23.
9. Porfir'ev M.A. Gromov V.E., Ivanov Yu.F., Popova N.A., Shlyarov V.V. Thin structure of long-length rails made of hypereutectoid steel after long-term operation. Novokuznetsk: Poligrafist; 2023:285. (In Russ.).

   Порфирьев М.А., Громов В.Е., Иванов Ю.Ф., Попова Н.А., Шляров В.В. Тонкая структура длинномерных рельсов из заэвтектоидной стали после длительной эксплуатации. Новокузнецк: Полиграфист; 2023:285.
10. Nikas D., Zhang X., Ahlstrom J. Evaluation of local strength via microstructural quantification in a pearlitic rail steel deformed by simultaneous compression and torsion. *Materials Science and Engineering: A*. 2018;737:341–347. https://doi.org/10.1016/j.msea.2018.09.067
11. Masoumi M., Sinatora A., Sietsma H.G. Role of microstructure and crystallographic orientation in fatigue crack failure analysis of a heavy haul railway rail. *Engineering Failure Analysis*. 2019;96:320–329. http://doi.org/10.1016/j.engfailanal.2018.10.022
12. Turan M.E., Aydin F., Sun Y., Cetin M. Residual stress measurement by strain gauge and X-ray diffraction method in different shaped rails. *Engineering Failure Analysis*. 2019;96: 525–529. https://doi.org/10.1016/j.engfailanal.2018.10.016
13. Li X.C., Ding H.H., Wang W.J., Guo J., Liu Q.Y., Zhou Z.R. Investigation on the relationship between microstructure and wear characteristic of rail materials. *Tribology International*. 2021; 163:107152. http://doi.org/10.1016/j.triboint.2021.107152
14. Kanematsu Y., Uehigashi N., Matsui M., Noguchi S. Influence of a decarburized layer on the formation of microcracks in railway rails: On-site investigation and twindisc study. *Wear*. 2022;504–505:204427. https://doi.org/10.1016/j.wear.2022.204427
15. Rong K.-J., Xiao Y.-L., Shen M.-X., Zhao H.-P., Wang W.-J., Xiong G.-Y. Influence of ambient humidity on the adhesion and damage behavior of wheel-rail interface under hot weather condition. *Wear*. 2021;486-487:204091. https://doi.org/10.1016/j.wear.2021.204091
16. Improvement of rail steels. *Zheleznye dorogi mira*. 2016;(1):74–76. (In Russ.).

   Совершенствование рельсовых сталей. *Железные дороги мира*. 2016;(1):74–76.
17. Dobuzhskaya A.B., Galitsyn G.A., Yunin G.N., Polevoi E.V., Yunusov A.M. Effect of chemical composition, microstructure and mechanical properties on the wear resistance of rail steel. *Steel in Translation*. 2020;50(12):906–910. https://doi.org/10.3103/S0967091220120037

   Добужская А.Б., Галицын Г.А., Юнин Г.Н., Полевой Е.В., Юнусов А.М. Влияние химического состава, микроструктуры и механических свойств на износостойкость рельсовой стали. *Сталь*. 2020;(12):52–55.
18. Wen J., Marteau J., Bouvier S., Risbet M., Cristofari F., Secorde P. Comparison of microstructure changes induced in two pearlitic rail steels subjected to a full-scale wheel/rail contact rig test. *Wear*. 2020;456-457:203354. http://doi.org/10.1016/j.wear.2020.203354
19. Hu Y., Guo L.C., Maiorino M., Liu J.P., Ding H.H., Lewis R., Meli E., Rindi A., Liu Q.Y., Wang W.J. Comparison of wear and rolling contact fatigue behaviours of bainitic and pearlitic rails under various rolling-sliding conditions. *Wear*.

2020;460-461:203455.
http://doi.org/10.1016/j.wear.2020.203455

20. Hu Y., Zhou L., Ding H.H., Lewis R., Liu Q.Y., Guo J., Wang W.J. Microstructure evolution of railway pearlitic wheel steels under rolling-sliding contact loading. *Tribology International*. 2021;154:106685.
http://doi.org/10.1016/j.triboint.2020.106685

21. Zhou L., Bai W., Han Z., Wang W., Hu Yu., Ding H., Lewis R., Meli E., Liu Q., Guo J. Comparison of the damage and microstructure evolution of eutectoid and hypereutectoid rail steels under a rolling-sliding contact. *Wear*. 2022;492-493:204233.
http://doi.org/10.1016/j.wear.2021.204233

22. Bai W., Zhou L., Wang P., Hu Y., Wang W., Ding H., Han Z., Xu X., Zhu M. Damage behavior of heavy-haul rail steels used from the mild conditions to harsh conditions. *Wear*. 2022;496-497:204290.
http://doi.org/10.1016/j.wear.2022.204290

23. Alwahdi F.A.M., Kapoor A., Franklin F.J. Subsurface microstructural analysis and mechanical properties of pearlitic rail steels in service. *Wear*. 2013;302(1-2):1453–1460.
http://doi.org/10.1016/j.wear.2012.12.058

24. Wang W.J., Lewis R., Yang B., Guo L.C., Liu Q.Y., Zhu M.H. Wear and damage transitions of wheel and rail materials under various contact conditions. *Wear*. 2016;362-363:146–152.
http://doi.org/10.1016/j.wear.2016.05.021

25. Pan R., Ren R., Zhao X., Chen C. Influence of microstructure evolution during the sliding wear of CL65 steel. *Wear*. 2018;400-401:169–176.
http://doi.org/10.1016/j.wear.2018.01.005

26. Egerton F.R. Physical Principles of Electron Microscopy. Basel: Springer International Publishing; 2016:196.
https://doi.org/10.1007/978-3-319-39877-8

27. Kumar C.S.S.R. Transmission Electron Microscopy. Characterization of Nanomaterials. New York: Springer; 2014:717.

28. Carter C.B., Williams D.B. Transmission Electron Microscopy: Diffraction, Imaging, and Spectrometry. Berlin: Springer International Publishing; 2016:518.
https://doi.org/10.1017/S1431927618000296

29. Popova N.A., Gromov V.E., Ivanov Yu.F., Porfir'ev M.A., Nikonenko E.L., Shlyarova Yu.A. Effect of long-term operation on the structural-phase state of hypereutectoid rail steel. *Materialovedenie*. 2023;(10):17–28. (In Russ.).
https://doi.org/10.31044/1684-579X-2023-0-10-17-28

Попова Н.А., Громов В.Е., Иванов Ю.Ф., Порфирьев М.А., Никоненко Е.Л., Шлярова Ю.А. Влияние длительной эксплуатации на структурно-фазовое состояние заэвтектоидной рельсовой стали. *Материаловедение*. 2023;(10):17–28. https://doi.org/10.31044/1684-579X-2023-0-10-17-28

30. Gol'dshtein M.I., Farber V.M. Dispersion Hardening of Steel. Moscow: Metallurgiya; 1979:208. (In Russ.).

Гольдштейн М.И., Фарбер В.М. Дисперсионное упрочнение стали. Москва: Металлургия; 1979:208.

31. Kozlov E.V., Koneva N.A. The nature of metal materials hardening. *Izvestiya vuzov. Fizika*. 2002;45(3):52–71. (In Russ.).

Козлов Э.В., Конева Н.А. Природа упрочнения металлических материалов. *Известия вузов. Физика*. 2002; 45(3):52–71.

32. Kozlov E.V., Malinovskaya V.A., Popova N.A. Quantitative assessment of hardening of nitrocemented steel 20Kh2N4A after low tempering. *Izvestiya. Ferrous Metallurgy*. 2006; 49(6):37–39. (In Russ.).

Козлов Э.В., Малиновская В.А., Попова Н.А. Количественная оценка упрочнения нитроцементованной стали 20Х2Н4А после низкого отпуска. *Известия вузов. Черная металлургия*. 2006;49(6):37–39.

Information about the Authors / Сведения об авторах

Natal'ya A. Popova, *Cand. Sci. (Eng.), Research Associate of the Scientific and Educational Laboratory "Nanomaterials and Nanotechnologies",* Tomsk State University of Architecture and Building
ORCID: 0000-0001-8823-4562
E-mail: natalya-popova-44@mail.ru

Viktor E. Gromov, *Dr. Sci. (Phys.-Math.), Prof., Head of the Chair of Science named after V.M. Finkel',* Siberian State Industrial University
ORCID: 0000-0002-5147-5343
E-mail: gromov@physics.sibsiu.ru

Aleksei B. Yur'ev, *Dr. Sci. (Eng.), Prof., Rector,* Siberian State Industrial University
ORCID: 0000-0002-9932-4755
E-mail: rector@sibsiu.ru

Efim A. Martusevich, *Cand. Sci. (Eng.), Research Associate of the Laboratory of Electron Microscopy and Image Processing,* Siberian State Industrial University
ORCID: 0000-0002-2335-7788
E-mail: program.pro666@gmail.com

Mikhail A. Porfir'ev, *Research Associate of Department of Scientific Researches,* Siberian State Industrial University
ORCID: 0000-0003-3602-5739
E-mail: mporf372@gmail.com

Наталья Анатольевна Попова, *к.т.н., научный сотрудник научно-учебной лаборатории «Наноматериалы и нанотехнологии»,* Томский государственный архитектурно-строительный университет
ORCID: 0000-0001-8823-4562
E-mail: natalya-popova-44@mail.ru

Виктор Евгеньевич Громов, *д.ф.-м.н., профессор, заведующий кафедрой естественнонаучных дисциплин им. проф. В.М. Финкеля,* Сибирский государственный индустриальный университет
ORCID: 0000-0002-5147-5343
E-mail: gromov@physics.sibsiu.ru

Алексей Борисович Юрьев, *д.т.н., профессор, ректор,* Сибирский государственный индустриальный университет
ORCID: 0000-0002-9932-4755
E-mail: rector@sibsiu.ru

Ефим Александрович Мартусевич, *к.т.н., научный сотрудник лаборатории электронной микроскопии и обработки изображений,* Сибирский государственный индустриальный университет
ORCID: 0000-0002-2335-7788
E-mail: program.pro666@gmail.com

Михаил Анатольевич Порфирьев, *научный сотрудник Управления научных исследований,* Сибирский государственный индустриальный университет
ORCID: 0000-0003-3602-5739
E-mail: mporf372@gmail.com

Contribution of the Authors

N. A. Popova – quantitative calculation of hardening mechanisms.
V. E. Gromov – formation of the article concept, discussion of the results, writing the article final version.
A. B. Yur'ev – discussion of the results, writing the article draft.

E. A. Martusevich – preparation of samples for TEM studies, processing of measurement results.
M. A. Porfir'ev – production of foils, participation in TEM studies, literary review.

Вклад авторов

Н. А. Попова – количественный расчет механизмов упрочнения.
В. Е. Громов – формирование концепции статьи, обсуждение результатов, написание окончательного варианта статьи.
А. Б. Юрьев – обсуждение результатов, написание чернового варианта статьи.
Е. А. Мартусевич – подготовка образцов для ПЭМ-исследований, обработка результатов измерений.
М. А. Порфирьев – изготовление фольг, участие в ПЭМ-исследованиях, обзор литературы.

Received 02.02.2024
Revised 19.02.2024
Accepted 29.03.2024

Поступила в редакцию 02.02.2024
После доработки 19.02.2024
Принята к публикации 29.03.2024